THE ARCHIVE OF MECHANICAL ENGINEERING

Vol. XLVII 2000 Number 3

Key words: *flight dynamics, stability*

ZDOBYSŁAW GORAJ), ADAM PRZEKOP*)*

FLIGHT DYNAMICS ANALYSIS OF A GLIDER IN SYMMETRICAL MOTION – THE CASE STUDY FOR PW-5

Dynamic stability analysis of the World Class Glider PW-5 has been presented. Glider was assumed to be a rigid body of three degrees of freedom – two linear displacements and one rotation – all in the plane of symmetry. Responses of the glider due to gust and deflection of elevator have been determined.

The Laplace transform has been applied to convert the differential equations into algebraic ones. The transformed algebraic equations, after a number of manipulations have been solved for the output variables. Partial-fraction expansions have been performed to obtain the inverse Laplace transforms from the Laplace transform table.

Although some restricting assumptions have been made (rigid body, small disturbances) the presented results are original and have not been presented before. The airworthiness regulations (JAR, FAR) do not require performing dynamic analysis in order the glider to be granted a Certificate of Airworthiness by the national aviation authority. To certificate the glider it is sufficient to prove static stability by means of in-flight tests. Flying qualities are qualitatively estimated basing on subjective opinions of the test pilots.

Symbols

$Axyz$ - body frame of reference, ($A = 0.25\ \bar{c}$; Ax - axis directed forward along mean aerodynamic chord; Az - axis perpendicular to Ax axis, downwards; Ay - axis along the right wing of the glider perpendicular to the Axz plane),

A - aspect ratio,

$\bar{c}$ - mean aerodynamic chord (MAC),

$\vec{F}_A$ - aerodynamic force,

*) *Warsaw University of Technology, Institute of Aeronauics and Applied Mechanics, Nowowiejska 24, 00-665 Warsaw, Poland; E-mail: goraj@meil.pw.edu. pl*

$\vec{f}_A$	-	disturbance of $\vec{F}_A$,
$\vec{g}$	-	acceleration due to gravity,
I_{yy}	-	moment of interia about Ay axis,
$\vec{K}_A$	-	angular momentum,
$\vec{M}_A$	-	pitching moment about point A,
$\vec{m}_A$	-	disturbance of $\vec{M}_A$,
m	-	mass of the glider,
P,Q,R	-	angular velocities around axes x, y, z, respectively,
p, q, r	-	disturbances of angular velocities P,Q,R, respectively,
$\vec{r}$	-	position of the mass centre of the glider,
$\overline{q}_1$	-	dynamic pressure in a steady, straight flight,
S	-	wing area,
S_h	-	tailplane area,
t	-	time,
U,V,W	-	components of $\vec{V}_P$ versus Ax, Ay and Az axes, respectively,
U_1,V_1,W_1	-	values of U,V,W in a steady, straight flight, respectively,
u, v, w	-	disturbances of linear velocities U,V,W, respectively,
$\vec{V}_P$	-	linear velocity of the glider,
x_c	-	location of the mass centre of the glider in the design frame of reference $Ax_d y_d z_d$ (Ax_d - directed backward along MAC; Az_d - directed upward, perpendicular to Ax_d; Ay_d - perpendicular to $Ax_d z_d$ plane versus right wing),
x_h	-	arm of tailplane, measured in the design frame of reference $Ax_d y_d z_d$,
δ_e	-	elevator deflection,
ε	-	angle of downwash,
Ψ,Θ,Φ	-	angles of yawing, pitching and banking,
Ψ_1,Θ_1,Φ_1	-	values of Ψ,Θ,Φ in a steady, straight flight, respectively,
ψ, θ, ϕ	-	disturbances of angels Ψ,Θ,Φ, respectively,
$\vec{\omega}$	-	angular velocity.

Aerodynamic coefficients denoted with subscript 1 refer to a steady, straight flight.

1. Introduction

For the past twenty five years, the airworthiness requirements have been significantly extended. Times when in-flight test programme could be completed in one day time are gone. Apart of the advances in computational methods, designers are usually reluctant to do excessive calculations – especially when referring to non-high-performance gliders. They have to accept a minimum demand which follows directly from airworthiness requirements but nothing more. At the same time, it can be very often heard from pilots that two gliders of comparable design have quite different flying and handling qualities.

Although a wide range of publications devoted to flight dynamic analysis (Roskam (1995), Cook (1995), Hancock (1997)) is available, no one relates specifically to gliders. It reflects a tendency to pay more attention to the performance of gliders (like the best glide ratio, for example) or strength and stiffness characteristics instead of flight dynamics and control characteristics.

Flight dynamics equations of motion used in this paper are written in the body frame of reference and have dimensional form. However, many aerodynamic phenomena are most conveniently explained in terms of dimensional aerodynamic coefficients, for example Ma, Re, C_L, dimensionless stability derivatives etc. The advantage of this approach is that the aerodynamic properties of a flying vehicle can be completely described in terms of dimensionless properties, being independent of structure geometry and flight condition, see Cook, 1995. However, the dimensionless equations of motion are of little use to-day other than as a means for explaining the origin of dimensionless derivatives. The important reason for such an approach is that stability derivatives are usually computed (or sometimes measured) in the wind frame of reference, and then are transformed to the body frame of reference. Such a transformation (having the tensor nature) is valid only for dimensional (not for dimensionless!) form of stability derivatives, see Cook 1995 & Goraj 1984.

2. Mathematical model

Flight dynamics equations of motion in the body frame of reference $Axyz$ (Fig.1) can be written as

$$m(\dot{\vec{V}}_P + \vec{\omega}\times\vec{V}_P) = m\vec{g} + \vec{F}_A , \tag{1}$$

$$\dot{\vec{K}} + \vec{\omega}\times\vec{K} = \vec{M}_A . \tag{2}$$

Scalar equations of motion for symmetrical flight derived from equations (1, 2) are as follows

$$m\left(\dot{U} + WQ\right) = mg_x + F_{A_x} , \tag{3a}$$

$$m\left(\dot{W} - UQ\right) = mg_z + F_{A_z} , \tag{3b}$$

$$I_{yy}\dot{Q} = M_A, \tag{3c}$$

where $g_x = -g\sin\Theta$; $g_z = g\cos\Theta$.

Let us consider a perturbed state flight condition, being defined as one for which all motion variables are defined relatively to a known steady state flight condition. The following substitutions are applied to all motion variables, forces and moment:

$U = U_1 + u$; $W = W_1 + w$; $Q = Q_1 + q$; $\Theta = \Theta_1 + \theta$;

$F_{Ax} = F_{Ax1} + f_{Ax}$; $F_{Az} = F_{Az1} + f_{Az}$; $M_A = M_{A1} + m_A$.

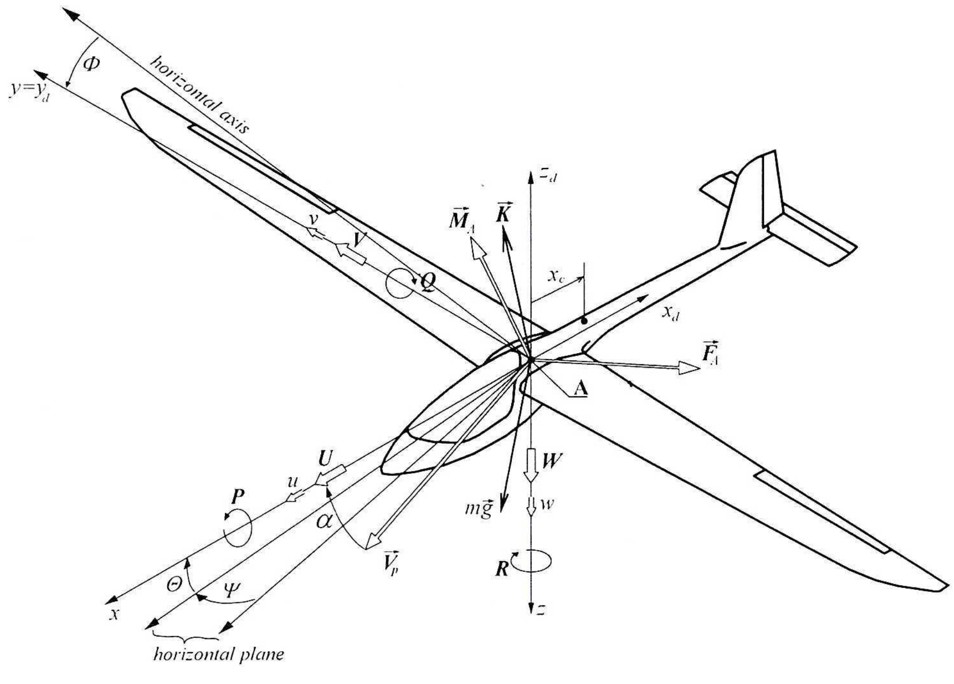

Fig.1 Body frame of reference Axyz; angles of yawing, pitching and banking; and aerodynamic forces and moments acting on sailplane

Assuming linear expansions of the trigonometric quantities one can obtain:

$\sin\Theta = \sin(\Theta_1 + \theta) \approx \sin\Theta_1 + \theta\cos\Theta_1$,

and

$\cos\Theta = \cos(\Theta_1 + \theta) \approx \cos\Theta_1 - \theta\sin\Theta_1$.

Steady state symmetrical flight equations of motion can be derived from (3) under the assumption that $\dot{U} = \dot{W} = \dot{Q} = Q = \theta = f_{Ax} = f_{Az} = m_A = 0$. Hence, the steady state equations have the form

$$mW_1Q_1 = -mg\sin\Theta_1 + F_{Ax1}, \tag{4a}$$

$$-mU_1Q_1 = mg\cos\Theta_1 + F_{Az1}, \tag{4b}$$

$$M_{A1} = 0. \tag{4c}$$

Subtracting eqs.(4) from corresponding eqs.(3) one can obtain perturbed equation of motion in the form

$$m(\dot{u} + W_1 q) = -mg\theta\cos\Theta_1 + f_{A_x}, \tag{5a}$$

$$m(\dot{w} - U_1 q) = -mg\theta\sin\Theta_1 + f_{A_z}, \tag{5b}$$

$$I_{yy}\dot{q} = m_A, \tag{5c}$$

known as the dynamic, small disturbance theory equations.

Equations (5) combined with kinematic equation

$$q = \dot{\theta}, \tag{5d}$$

describe disturbed state of flight around steady, straight flight trajectory, inclined to the horizontal axis on angle Θ_1. Assume that steady flight is disturbed by a small elevator deflection. Additional (disturbed) aerodynamic forces and moments can be written as functions of aerodynamic derivatives

$$f_{A_x} = \frac{\partial F_{A_x}}{\partial\left(\frac{u}{U_1}\right)}\left(\frac{u}{U_1}\right) + \frac{\partial F_{A_x}}{\partial\alpha}\alpha + \frac{\partial F_{A_x}}{\partial\left(\frac{\dot{\alpha}\bar{c}}{2U_1}\right)}\left(\frac{\dot{\alpha}\bar{c}}{2U_1}\right) + \frac{\partial F_{A_x}}{\partial\left(\frac{q\bar{c}}{2U_1}\right)}\left(\frac{q\bar{c}}{2U_1}\right) + \frac{\partial F_{A_x}}{\partial\delta_e}\delta_e, \tag{6a}$$

$$f_{A_z} = \frac{\partial F_{A_z}}{\partial\left(\frac{u}{U_1}\right)}\left(\frac{u}{U_1}\right) + \frac{\partial F_{A_z}}{\partial\alpha}\alpha + \frac{\partial F_{A_z}}{\partial\left(\frac{\dot{\alpha}\bar{c}}{2U_1}\right)}\left(\frac{\dot{\alpha}\bar{c}}{2U_1}\right) + \frac{\partial F_{A_z}}{\partial\left(\frac{q\bar{c}}{2U_1}\right)}\left(\frac{q\bar{c}}{2U_1}\right) + \frac{\partial F_{A_z}}{\partial\delta_e}\delta_e, \tag{6b}$$

$$m_A = \frac{\partial M_A}{\partial\left(\frac{u}{U_1}\right)}\left(\frac{u}{U_1}\right) + \frac{\partial M_A}{\partial\alpha}\alpha + \frac{\partial M_A}{\partial\left(\frac{\dot{\alpha}\bar{c}}{2U_1}\right)}\left(\frac{\dot{\alpha}\bar{c}}{2U_1}\right) + \frac{\partial M_A}{\partial\left(\frac{q\bar{c}}{2U_1}\right)}\left(\frac{q\bar{c}}{2U_1}\right) + \frac{\partial M_A}{\partial\delta_e}\delta_e. \tag{6c}$$

These disturbances can be presented in a vector-matrix notation as follow

$$\begin{Bmatrix} \dfrac{f_{A_x}}{\bar{q}_1 S} \\ \dfrac{f_{A_z}}{\bar{q}_1 S} \\ \dfrac{m_A}{\bar{q}S\bar{c}} \end{Bmatrix} = \begin{array}{|c|c|c|c|c|} \hline -(C_{D_u} + 2C_{D_1}) & (-C_{D_\alpha} + 2C_{L_1}) & -C_{D_{\dot{\alpha}}} & -C_{D_q} & -C_{D_{\delta_e}} \\ \hline -(C_{L_u} + 2C_{L_1}) & -(C_{L_\alpha} + 2C_{D_1}) & -C_{L_{\dot{\alpha}}} & -C_{L_q} & -C_{L_{\delta_e}} \\ \hline (C_{m_u} + 2C_{m_1}) & C_{m_\alpha} & C_{m_{\dot{\alpha}}} & C_{m_q} & C_{L_{\delta_e}} \\ \hline \end{array} \begin{Bmatrix} \dfrac{u}{U_1} \\ \alpha \\ \dfrac{\dot{\alpha}\bar{c}}{2U_1} \\ \dfrac{q\bar{c}}{2U_1} \\ \delta_e \end{Bmatrix} \tag{7}$$

where:

$$C_{D_U} = \frac{\partial C_D}{\partial\left(\dfrac{u}{U_1}\right)}, \quad C_{L_{\dot\alpha}} = \frac{\partial C_L}{\partial\left(\dfrac{\dot\alpha\ \bar c}{2U_1}\right)}, \qquad C_{m_{\delta_e}} = \frac{\partial C_m}{\partial \delta_e} \quad \text{etc.}$$

When disturbances are involved by gust, the symbol δ_e, denoting deflection of elevator, should be replaced with an increment of angle of attack $\Delta\alpha_g$, and stability derivatives $C_{D_{\delta_e}}$, $C_{L_{\delta_e}}$, $C_{m_{\delta_e}}$ at the last column of matrix in equation (7) have to be replaced with C_{D_α}, C_{L_α}, C_{m_α}, respectively.

Modified dimensional equations ((4a, 4b) divided by m and (4c) divided by I_{yy}) take the form

- for the small-disturbances of motion involved by elevator deflection

$$\dot u = -g\theta\cos\theta_1 + X_u u + X_\alpha \alpha + X_{\delta_e}\delta_e, \tag{8a}$$

$$U_1\dot\alpha - U_1\dot\theta = -q\theta\sin\theta_1 + Z_u u + Z_\alpha\alpha + Z_{\dot\alpha}\dot\alpha + Z_q\dot\theta + Z_{\delta_e}\delta_e, \tag{8b}$$

$$\dot\theta = M_u u + M_\alpha\alpha + M_{\dot\alpha}\dot\alpha + M_q\dot\theta + M_{\delta_e}\delta_e. \tag{8c}$$

- for the small-disturbances of motion involved by vertical gust

$$\dot u = -g\theta\cos\theta_1 + X_u u + X_\alpha \alpha + X_\alpha\Delta\alpha_g, \tag{9a}$$

$$U_1\dot\alpha - U_1\dot\theta = -q\theta\sin\theta_1 + Z_u u + Z_\alpha\alpha + Z_{\dot\alpha}\dot\alpha + Z_q\dot\theta + Z_\alpha\Delta\alpha_g, \tag{9b}$$

$$\dot\theta = M_u u + M_\alpha\alpha + M_{\dot\alpha}\dot\alpha + M_q\dot\theta + M_\alpha\Delta\alpha_g. \tag{9c}$$

Rewriting equations (8, 9) in such a way that disturbances due to either elevator deflection or gust are placed on the right hand side of equations, one can obtain

$$\begin{bmatrix} (s - X_u) & -X_\alpha & g\cos\theta_1 \\ -Z_u & \{s(U_1 - Z_{\dot\alpha}) - Z_\alpha\} & \{-(Z_q + U_1)s + g\sin\theta_1\} \\ -M_u & -(M_{\dot\alpha}s + M_\alpha) & (s^2 - M_q s) \end{bmatrix} \begin{Bmatrix} \dfrac{u(s)}{\delta_e(s)} \\ \dfrac{\alpha(s)}{\delta_e(s)} \\ \dfrac{\theta(s)}{\delta_e(s)} \end{Bmatrix} = \begin{Bmatrix} X_{\delta_e} \\ Z_{\delta_e} \\ M_{\delta_e} \end{Bmatrix}, \tag{10}$$

and

$$\begin{bmatrix} (s-X_u) & -X_\alpha & g\cos\theta_1 \\ -Z_u & \{s(U_1-Z_{\dot\alpha})-Z_\alpha\} & \{-(Z_q+U_1)s+g\sin\theta_1\} \\ -M_u & -(M_{\dot\alpha}s+M_\alpha) & (s^2-M_q s) \end{bmatrix} \begin{Bmatrix} \dfrac{u(s)}{\Delta\alpha_g(s)} \\ \dfrac{\alpha(s)}{\Delta\alpha_g(s)} \\ \dfrac{\theta(s)}{\Delta\alpha_g(s)} \end{Bmatrix} = \begin{Bmatrix} X_\alpha \\ Z_\alpha \\ M_\alpha \end{Bmatrix}. \tag{11}$$

Transforms found from equations (10, 11) are

- for the small-disturbances of motion involved by elevator deflection

$$\frac{u(s)}{\delta_e(s)} = \frac{\begin{vmatrix} X_{\delta_e} & -X_\alpha & g\cos\theta_1 \\ Z_{\delta_e} & \{s(U_1-Z_{\dot\alpha})-Z_\alpha\} & \{-(Z_q+U_1)s+g\sin\theta_1\} \\ M_{\delta_e} & -\{M_{\dot\alpha}s+M_\alpha\} & (s^2-M_q s) \end{vmatrix}}{\begin{vmatrix} (s-X_u) & -X_\alpha & g\cos\theta_1 \\ -Z_u & \{s(U_1-Z_{\dot\alpha})-Z_\alpha\} & \{-(Z_q+U_1)s+g\sin\theta_1\} \\ -M_u & -\{M_{\dot\alpha}s+M_\alpha\} & (s^2-M_q s) \end{vmatrix}} = \frac{N_u}{\bar{D}_1}, \tag{12}$$

$$\frac{\alpha(s)}{\delta_e(s)} = \frac{\begin{vmatrix} (s-X_u) & X_{\delta_e} & g\cos\theta_1 \\ -Z_u & Z_{\delta_e} & \{-(Z_q+U_1)s+g\sin\theta_1\} \\ -M_u & M_{\delta_e} & (s^2-M_q s) \end{vmatrix}}{\begin{vmatrix} (s-X_u) & -X_\alpha & g\cos\theta_1 \\ -Z_u & \{s(U_1-Z_{\dot\alpha})-Z_\alpha\} & \{-(Z_q+U_1)s+g\sin\theta_1\} \\ -M_u & -\{M_{\dot\alpha}s+M_\alpha\} & (s^2-M_q s) \end{vmatrix}} = \frac{N_\alpha}{\bar{D}_1}, \tag{13}$$

$$\frac{\theta(s)}{\delta_e(s)} = \frac{\begin{vmatrix} (s-X_u) & -X_\alpha & X_{\delta_e} \\ -Z_u & \{s(U_1-Z_{\dot\alpha})-Z_\alpha\} & Z_{\delta_e} \\ -M_u & -\{M_{\dot\alpha}s+M_\alpha\} & M_{\delta_e} \end{vmatrix}}{\begin{vmatrix} (s-X_u) & -X_\alpha & g\cos\theta_1 \\ -Z_u & \{s(U_1-Z_{\dot\alpha})-Z_\alpha\} & \{-(Z_q+U_1)s+g\sin\theta_1\} \\ -M_u & -\{M_{\dot\alpha}s+M_\alpha\} & (s^2-M_q s) \end{vmatrix}} = \frac{N_\theta}{\bar{D}_1}, \tag{14}$$

and for the small-disturbances of motion involved by vertical gust

$$\frac{u(s)}{\Delta\alpha_g(s)} = \frac{\begin{vmatrix} X_\alpha & -X_\alpha & g\cos\theta_1 \\ Z_\alpha & \{s(U_1 - Z_{\dot\alpha}) - Z_\alpha\} & \{-(Z_q + U_1)s + g\sin\theta_1\} \\ M_\alpha & -\{M_{\dot\alpha}s + M_\alpha\} & (s^2 - M_q s) \end{vmatrix}}{\begin{vmatrix} (s - X_u) & -X_\alpha & g\cos\theta_1 \\ -Z_u & \{s(U_1 - Z_{\dot\alpha}) - Z_\alpha\} & \{-(Z_q + U_1)s + g\sin\theta_1\} \\ -M_u & -\{M_{\dot\alpha}s + M_\alpha\} & (s^2 - M_q s) \end{vmatrix}} = \frac{N_u}{\bar{D}_1}, \quad (15)$$

$$\frac{\alpha(s)}{\Delta\alpha_g(s)} = \frac{\begin{vmatrix} (s - X_u) & X_\alpha & g\cos\theta_1 \\ -Z_u & Z_\alpha & \{-(Z_q + U_1)s + g\sin\theta_1\} \\ -M_u & M_\alpha & (s^2 - M_q s) \end{vmatrix}}{\begin{vmatrix} (s - X_u) & -X_\alpha & g\cos\theta_1 \\ -Z_u & \{s(U_1 - Z_{\dot\alpha}) - Z_\alpha\} & \{-(Z_q + U_1)s + g\sin\theta_1\} \\ -M_u & -\{M_{\dot\alpha}s + M_\alpha\} & (s^2 - M_q s) \end{vmatrix}} = \frac{N_\alpha}{\bar{D}_1}, \quad (16)$$

$$\frac{\theta(s)}{\Delta\alpha_g(s)} = \frac{\begin{vmatrix} (s - X_u) & -X_\alpha & X_\alpha \\ -Z_u & \{s(U_1 - Z_{\dot\alpha}) - Z_\alpha\} & Z_\alpha \\ -M_u & -\{M_{\dot\alpha}s + M_\alpha\} & M_\alpha \end{vmatrix}}{\begin{vmatrix} (s - X_u) & -X_\alpha & g\cos\theta_1 \\ -Z_u & \{s(U_1 - Z_{\dot\alpha}) - Z_\alpha\} & \{-(Z_q + U_1)s + g\sin\theta_1\} \\ -M_u & -\{M_{\dot\alpha}s + M_\alpha\} & (s^2 - M_q s) \end{vmatrix}} = \frac{N_\theta}{\bar{D}_1}, \quad (17)$$

where

$$\bar{D}_1 = A_1 s^4 + B_1 s^3 + C_1 s^2 + D_1 s + E_1$$

$$A_1 = U_1 - Z_{\dot\alpha}$$

$$B_1 = -(U_1 - Z_{\dot\alpha})(X_u + M_q) - Z_\alpha - M_{\dot\alpha}(U_1 + Z_q)$$

$$C_1 = X_u\left\{M_q\left(U_1 - Z_{\dot\alpha}\right) + Z_\alpha + M_{\dot\alpha}\left(U_1 + Z_q\right)\right\} + M_q Z_\alpha - Z_u X_\alpha + M_{\dot\alpha} g\sin\theta_1 +$$
$$- M_\alpha\left(U_1 + Z_q\right)$$
$$D_1 = g\sin\theta_1\left\{M_\alpha - M_{\dot\alpha} X_u\right\} + g\cos\theta_1\left\{Z_u M_{\dot\alpha} + M_u\left(U_1 - Z_{\dot\alpha}\right)\right\} +$$
$$+ M_u\left\{-X_\alpha\left(U_1 + Z_q\right)\right\} + Z_u X_\alpha M_q + X_u\left\{M_\alpha\left(U_1 + Z_q\right) - M_q Z_\alpha\right\}$$
$$E_1 = g\cos\theta_1\left\{M_\alpha Z_u - Z_\alpha M_u\right\} + g\sin\theta_1\left\{M_u X_\alpha - X_u M_\alpha\right\}$$

$$N_u = A_u s^3 + B_u s^2 + C_u s + D_u$$
$$A_u = X_{\delta_e}\left(U_1 - Z_{\dot\alpha}\right)$$
$$B_u = -X_{\delta_e}\left\{\left(U_1 - Z_{\dot\alpha}\right)M_q + Z_\alpha + M_{\dot\alpha}\left(U_1 + Z_q\right) + Z_{\delta_e} X_\alpha\right\}$$
$$C_u = X_{\delta_e}\left\{M_q Z_\alpha + M_{\dot\alpha} g\sin\theta_1 - M_\alpha\left(U_1 + Z_q\right)\right\} + Z_{\delta_e}\left\{-M_{\dot\alpha} g\cos\theta_q - X_\alpha M_q\right\} +$$
$$+ M_{\delta_e}\left\{X_\alpha\left(U_1 + Z_q\right) - \left(U_1 - Z_{\dot\alpha}\right) g\cos\theta_1\right\}$$
$$D_u = X_{\delta_e} M_\alpha g\sin\theta_1 - Z_{\delta_e} M_\alpha g\cos\theta_1 + M_{\delta_e}\left(Z_\alpha g\cos\theta_1 - X_\alpha g\sin\theta_1\right)$$

$$N_\alpha = A_\alpha s^3 + B_\alpha s^2 + C_\alpha s + D_\alpha$$
$$A_\alpha = Z_{\delta_e}$$
$$B_\alpha = X_{\delta_e} Z_u + Z_{\delta_e}\left\{-M_q - X_u\right\} + M_{\delta_e}\left(U_1 + Z_q\right)$$
$$C_\alpha = X_{\delta_e}\left\{\left(U_1 + Z_q\right)M_u - M_q Z_u\right\} + Z_{\delta_e} M_q X_u + M_{\delta_e}\left\{-g\sin\theta_1 - \left(U_1 + Z_q\right)X_u\right\}$$
$$D_\alpha = -X_{\delta_e} M_u g\sin\theta_1 + Z_{\delta_e} M_u g\cos\theta_1 + M_{\delta_e}\left(X_u g\sin\theta_1 - Z_u g\cos\theta_1\right)$$

$$N_\theta = A_\theta s^2 + B_\theta s + C_\theta$$
$$A_\theta = Z_{\delta_e} M_{\dot\alpha} + M_{\delta_e}\left(U_1 - Z_{\dot\alpha}\right)$$
$$B_\theta = X_{\delta_e}\left\{Z_u M_{\dot\alpha} + \left(U_1 - Z_{\dot\alpha}\right)M_u\right\} + Z_{\delta_e}\left\{M_\alpha - M_{\dot\alpha} X_u\right\} +$$
$$+ M_{\delta_e}\left\{-Z_\alpha - \left(U_1 - Z_{\dot\alpha}\right)X_u\right\}$$
$$C_\theta = X_{\delta_e}\left\{M_\alpha Z_u - Z_\alpha M_u\right\} + Z_{\delta_e}\left\{-M_\alpha X_u + X_\alpha M_u\right\} +$$
$$+ M_{\delta_e}\left\{Z_\alpha X_u - X_\alpha Z_u\right\}$$

$$N_u = A_u s^3 + B_u s^2 + C_u s + D_u$$
$$A_u = X_\alpha\left(U_1 - Z_{\dot\alpha}\right)$$
$$B_u = -X_\alpha\left\{\left(U_1 - Z_{\dot\alpha}\right)M_q + Z_\alpha + M_{\dot\alpha}\left(U_1 + Z_q\right) + Z_\alpha X_\alpha\right\}$$

$$C_u = X_\alpha \left\{ M_q Z_\alpha + M_{\dot\alpha} g \sin\theta_1 - M_\alpha \left(U_1 + Z_q \right) \right\} + Z_\alpha \left\{ -M_{\dot\alpha} g \cos\theta_q - X_\alpha M_q \right\} +$$
$$+ M_\alpha \left\{ X_\alpha \left(U_1 + Z_q \right) - \left(U_1 - Z_{\dot\alpha} \right) g \cos\theta_1 \right\}$$
$$D_u = X_\alpha M_\alpha g \sin\theta_1 - Z_\alpha M_\alpha g \cos\theta_1 + M_\alpha \left(Z_\alpha g \cos\theta_1 - X_\alpha g \sin\theta_1 \right)$$

$$N_\alpha = A_\alpha s^3 + B_\alpha s^2 + C_\alpha s + D_\alpha$$
$$A_\alpha = Z_\alpha$$
$$B_\alpha = X_\alpha Z_u + Z_\alpha \left\{ -M_q - X_u \right\} + M_\alpha \left(U_1 + Z_q \right)$$
$$C_\alpha = X_\alpha \left\{ \left(U_1 + Z_q \right) M_u - M_q Z_u \right\} + Z_\alpha M_q X_u + M_\alpha \left\{ -g \sin\theta_1 - \left(U_1 + Z_q \right) X_u \right\}$$
$$D_\alpha = -X_\alpha M_u g \sin\theta_1 + Z_\alpha M_u g \cos\theta_1 + M_\alpha \left(X_u g \sin\theta_1 - Z_u g \cos\theta_1 \right)$$

$$N_\theta = A_\theta s^2 + B_\theta s + C_\theta$$
$$A_\theta = Z_\alpha M_{\dot\alpha} + M_\alpha \left(U_1 - Z_{\dot\alpha} \right)$$
$$B_\theta = X_\alpha \left\{ Z_u M_{\dot\alpha} + \left(U_1 - Z_{\dot\alpha} \right) M_u \right\} + Z_\alpha \left\{ M_\alpha - M_{\dot\alpha} X_u \right\} +$$
$$+ M_\alpha \left\{ -Z_\alpha - \left(U_1 - Z_{\dot\alpha} \right) X_u \right\}$$
$$C_\theta = X_\alpha \left\{ M_\alpha Z_u - Z_\alpha M_u \right\} + Z_\alpha \left\{ -M_\alpha X_u + X_\alpha M_u \right\} +$$
$$+ M_\alpha \left\{ Z_\alpha X_u - X_\alpha Z_u \right\}$$

Having formulae for transfer functions in the form of (12-14) and (15-17), one can find a response of the glider to various forms of input involved by either deflection of elevator or gust.

3. Numerical calculations

Calculations have been performed taking the PW-5 - World Class Glider as an example. Technical data were obtained from [5], [6], [8], [9], [10]. It was assumed that the glider was initially in the steady, straight flight inclined to the level at the negative pitch angle Θ_1.

The following data have been used

- geometrical and mass parameters

$S = 10.16\ \text{m}^2$; $\quad S_h = 1.20\ \text{m}^2$; $\quad \bar{c} = 0{,}798\ \text{m}$; $\quad A = 17.779$;

$\dfrac{x_h - x_c}{\bar{c}} = 4.538$; $\quad I_{yy} = 480\ kg \cdot m^2 \quad$ for $\quad \bar{x}_c = \dfrac{x}{\bar{c}} = 0.315$;

- aerodynamic characteristics

$C_{L_1}=0.668$; $C_{L_\alpha}=5.9078\left(rad^{-1}\right)$; $C_{L_U}=0\left(rad^{-1}\right)$; $C_{L_{\alpha h}}=3.723\left(rad^{-1}\right)$;

$C_{D_1}=0.021$; $C_{D_\alpha}=0.1637\left(rad^{-1}\right)$; $C_{m_1}=0\left(rad^{-1}\right)$; $C_{m_U}=0\left(rad^{-1}\right)$;

$\frac{d\varepsilon}{d\alpha}=0.250$;

$$C_{m_\alpha}=\frac{\partial C_{mbh}}{\partial\alpha}-C_{L_{\alpha h}}\frac{S_h}{S}(\bar{x}_h-\bar{x}_c)\left(1-\frac{d\varepsilon}{d\alpha}\right)=-1.138\left(rad^{-1}\right),$$

$$C_{L_{\dot\alpha}}=2C_{L_{\alpha h}}\frac{d\varepsilon}{d\alpha}(\bar{x}_h-\bar{x}_c)\frac{S_h}{S}=0.9968\left(rad^{-1}\right),$$

$$C_{m_{\dot\alpha}}=-2C_{L_{\alpha h}}\frac{d\varepsilon}{d\alpha}\frac{S_h}{S}(\bar{x}_h-\bar{x}_c)^2=-4.5235\left(rad^{-1}\right),$$

$$C_{L_q}=2C_{L_{\alpha h}}(\bar{x}_h-\bar{x}_c)\frac{S_h}{S}=3.9872\left(rad^{-1}\right),$$

$$C_{m_q}=-2C_{L_{\alpha h}}\frac{S_h}{S}(\bar{x}_h-\bar{x}_c)^2=-18.094\left(rad^{-1}\right).$$

Characteristic equation for denominator in equation (12) was evaluated to the form of polynomial, and then to a product of monomials in the form

$$\det\begin{bmatrix} s+0.0247 & -2.3645 & 9.77 \\ 0.7843 & 25.2335\cdot s+87.016 & -24.066\cdot s+0.855 \\ 0 & 0.4668\cdot s+7.3584 & s^2+1.867\cdot s \end{bmatrix}=$$
$$=25.2335\cdot s^4+145.9842\cdot s^3+344.5919\cdot s^2+9.1247\cdot s+56.2292=$$
$$=(s+2.914+2.291i)(s+2.914-2.291i)(s-0.021+0.402i)(s-0.021-0.402i) \tag{18}$$

Poles of denominator can be found as eigenvalues of the characteristic matrix corresponding to matrix equations (10, 11). Location of poles in $G(s)$ plane determine dynamic stability of the glider. Eigenvalues of the characteristic matrix determine a response of the glider and give the undamped natural frequencies ω and dimensionless damping ratios ξ. Calculations were done by means of three different methods:

1) computing the roots of characteristic equation (18),
2) using STB-9702 software package [7] (eigenvalues of the characteristic matrix have been found),
3) applying algorithm presented by Roskam [1].

The obtained results are presented in Tab. 1 (roots of characteristic equation (18) and eigenvalues of the characteristic matrix from equation (10) are exactly the same and were placed in columns 2 and 3 in Tab. 1.

Table 1.

Undamped natural frequencies and damping ratios

Mode	According to [7] (STB-9702)		According to [1] (Roskam)		Difference	
	ω [Hz]	ξ [-]	ω [Hz]	ξ [-]	ω	ξ
Short period	3.798	0.767	3.707	0.786	-2.4%	+2.5%
Phugoid	0.462	-0.059	0.401	-0.052	-13.2%	+11.9%

The obtained results show that the PW-5 glider has a convergent short period mode (disturbances are damped) and divergent phugoid mode (disturbances are increasing). That kind of instability does not have an acute character and the effect of increase of an amplitude of oscillation allows the pilot to react easily. The short period mode of oscillation in the most unfavorable case of the aft limit of the center of gravity location is damped well – time to the half of amplitude is of order 4 sec. The influence of the location of the center of gravity on the dynamic stability is shown in Tab. 2.

Table 2.

Influence of location of the center of gravity on dynamic stability

Location of CG in percents of MAC	Time-to-double of amplitude for phugoid mode [sec]	Time-to-half of amplitude for short period mode [sec]
20,0 (forward limit)	40.7	3.3
31,5 (middle)	25.1	3.7
43,0 (aft limit)	22.6	4.1

For system in series, the overall transfer function $G(s)$ is the product of the transfer functions $G_i(s)$ of the separate systems

$$G(s)=G_1(s)\cdot G_1(s)\cdot\ldots\ldots\cdot G_i(s)\cdot\ldots\ldots \tag{19}$$

Thus, the overall frequency-response function is the product of the frequency-response functions of the separate systems

$$G(j\omega)=G_1(j\omega)\cdot G_1(j\omega)\cdot\ldots\ldots\cdot G_i(j\omega)\cdot\ldots\ldots \tag{20}$$

and thus one obtains

$$|G(j\omega)|\angle\Phi=G(j\omega_1)\angle\Phi_1\times G(j\omega_2)\angle\Phi_2\times\ldots\ldots\times G(j\omega_i)\angle\Phi_i\times\ldots\ldots \tag{21}$$

From (21) it can be shown [11] that

$$|G(j\omega)| = |G(j\omega_1)| \cdot |G(j\omega_2)| \cdot \ldots\ldots\ldots \cdot |G(j\omega_i)| \cdot \ldots\ldots\ldots\ldots \tag{22}$$

and

$$\Phi = \Phi_1 + \Phi_2 + \ldots\ldots + \Phi_i + \ldots\ldots \tag{23}$$

Graphs of magnitude in dB ($dB = 20\log|G(j\omega)|$) plotted against the logarithm of the frequency and of the phase plotted against the logarithm of the frequency are usually called as the Bode plots. A number of Bode plots has been created basing on the tranfer functions (12-14) and (15-17).

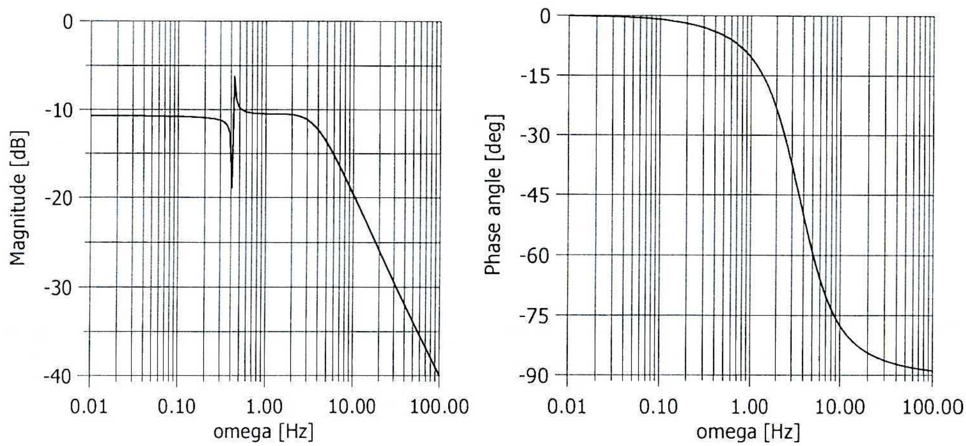

Fig. 2. Magnitude [dB] and phase angle [deg] of the angle of attack against the frequency of gust

Fig. 2 presents a response of the glider (in the form of Bode plots) after a gust resulting in an increase of the angle of attack. Bode plots in Fig. 2 are based on the transfer function (24) and correspond to the general form of transfer in the form (16):

$$G(\omega) = \frac{(i\omega + 3.973)(i\omega - 0.012 + 0.403i)(i\omega + 0.012 + 0.403i)}{(s + 2.914 + 2.291i)(s + 2.914 - 2.291i)(s - 0.021 + 0.402i)(s - 0.021 - 0.402i)} \tag{24}$$

Bode plots in Fig. 2 show that the steady response has a maximum amplitude when the frequency is in the range of that between the phugoid and short period natural frequencies ($0.40 < \omega < 3.71\,\text{Hz}$). A little bit smaller magnitude corresponds to the frequency of phugoid mode ($\omega < 0.40\,\text{Hz}$). At higher frequencies (above the short period natural frequency, $\omega > 3.71\,\text{Hz}$), sudden decrease in the magnitude can be observed. It means that the glider is almost insensitive to such suddenly changing impuls. However, that observation has rather an academic meaning, because disturbances of such a kind are very unlikely in the real atmosphere. Such disturbances can take place only during take-off or landing and can be caused by the airfield roughness.

Phase angle diagram in Fig. 2 shows that disturbances exciting the phugoid mode ($\omega < 1$ Hz) create a small phase angle, not exceeding 10°. In the range of frequencies between *1* and *10* Hz one can be observe that the delay increases up to 80° and after that the phase delay converges to the asymptotic value of 90°. Low frequency of disturbances corresponds to the thermal air currents, which are usually fuzzy ('washed out'), so the perturbations of angle of attack are small. As a consequence, pilot has more time to react. If a disturbance is stronger, the phase delay is bigger, and the magnitude is smaller.

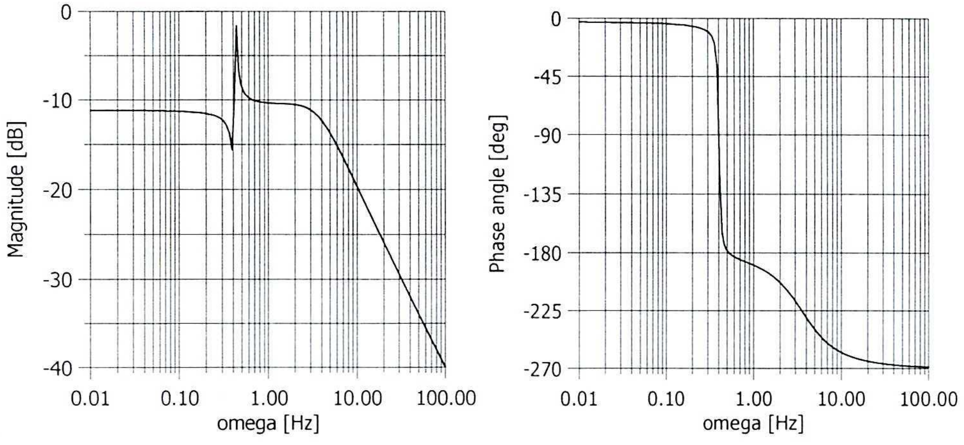

Fig.3. Magnitude [dB] and phase angle [deg] of the angle of attack against the frequency of elevator deflection

Fig. 3 presents the response of the glider (in the form of Bode plots) after an elevator deflection. Bode plots in Fig. 3 are based on the transfer function (25) and correspond to the general form of transfer function in the form (13):

$$G(\omega)=\frac{(i\omega+3.981)(i\omega-0.012+0.403i)(i\omega+0.012+0.403i)}{(s+2.914+2.291i)(s+2.914-2.291i)(s-0.021+0.402i)(s-0.021-0.402i)} \tag{25}$$

Bode plots in Fig. 3 show that the steady response has a maximum amplitude if the frequency is in the range of frequency between that of phugoid and short period mode ($0.40<\omega<3.71$ Hz). A little bit smaller magnitude corresponds to the frequency of phugoid mode ($\omega<0.40$ Hz). At higher frequencies (above the short period natural frequency $\omega>3.71$ Hz) sudden decrease in the magnitude can be observed. It means that the glider is almost insensitive to such a sudden deflections of an elevator. A very common mistake which happens to the beginner pilots is the tendency to control the glider or plane using 'impulse' motions, i.e. by means of very frequent but short (in time) deflections of control surfaces. Magnitudes against frequencies shown in Fig. 3 confirm that such a practice is irrational and inefficient. However, low frequency control using smooth, longer time acting deflection can be found as an efficient and proper control habituation. It is worthy to notice that magnitude due to elevator deflection is of a very similar shape as the magnitude due to gust disturbance.

Fig. 3 shows that at low frequencies ($\omega < 0.4$ Hz) the delay in phase angle is closed to 0°. In the range of frequencies near to the natural frequency of phugoid mode ($\omega \approx 0.40$ Hz) it can be observed that the delay increases suddenly to the value of order 180°. From this point, further decrease is not so violent and continues up to the natural frequency of short period mode ($\omega \approx 3.71$ Hz). After that the phase delay begins its second sudden decrease which lasts up to frequency of about *15* Hz. At the end, the phase delay converges to the asymptotic value of 270°. This almost 'ramp shape' can be recognized as a typical phase plot for conventional airplane or glider.

4. Response of the system to an aperiodical input signal

In Chapter 3 the steady responses of the system to periodical disturbances have been, presented. Responses to aperiodic input signals due to the elevator deflection and gusts have been investigated next. Input signals have been selected in order to have the response function in the so-called closed form, mathematically as simple as possible [4]. Time functions have been found by inverse Laplace transform.

Numerical calculations have been done for five different input signals. Each of them is shown in Tab. 3 (disturbances due to gust, Fig. 4-8) and in Tab. 4 (disturbances due to elevator deflection, Fig. 9-13). These figures contain characteristic impulses (as separate plots) and three degrees of freedom response having: angle of attack ([*deg*], solid line), pitching angle ([*deg*], dash-dotted line) and disturbance of forward speed ([*km/h*], dashed line).

Table 3.

Disturbances due to gust

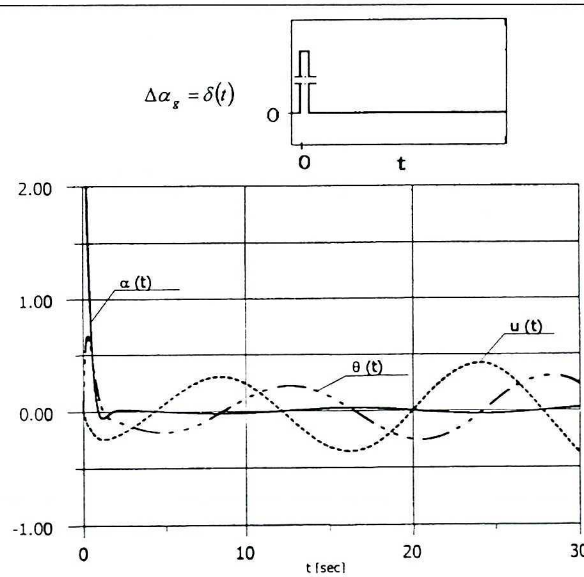

Fig. 4. Excitation by Dirac impulse

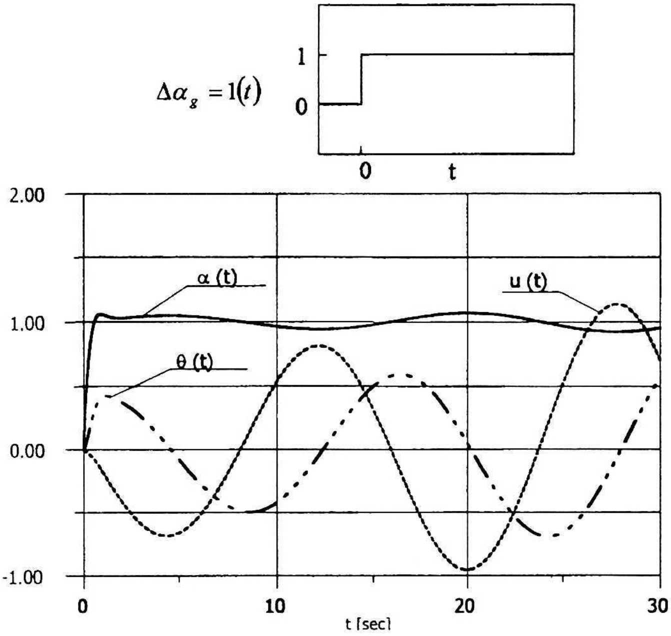

Fig. 5. Excitation by Heviside function

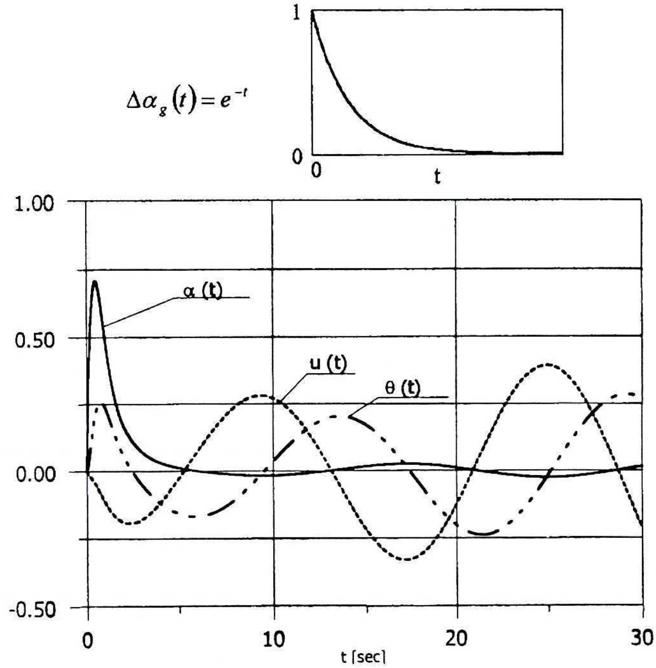

Fig. 6. Exponential impulse

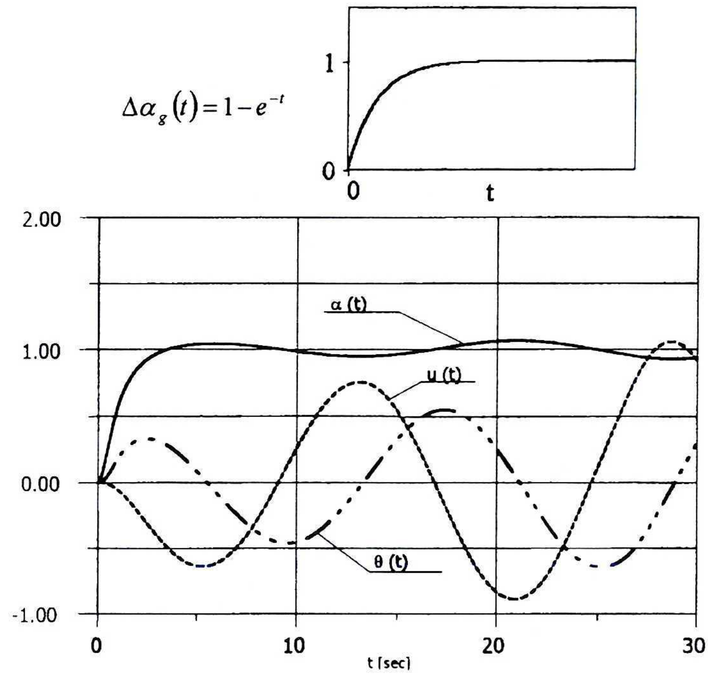

Fig. 7. Unit minus exponential impulse

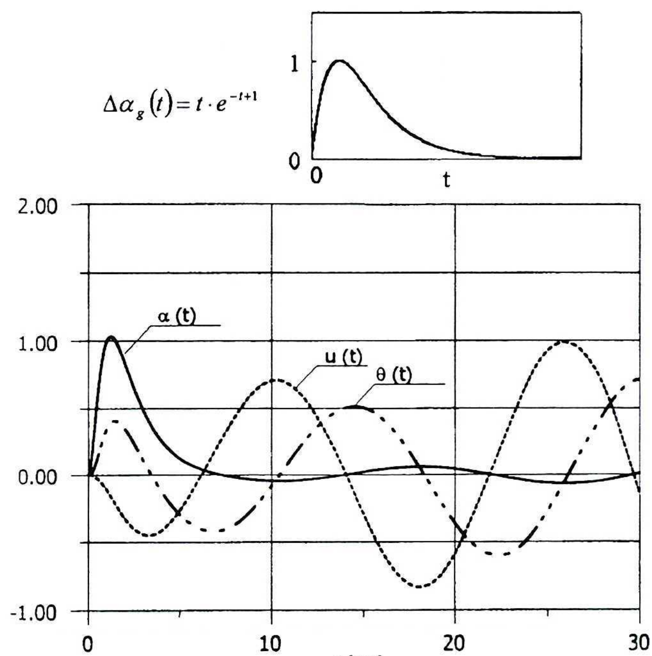

Fig. 8. Complex impulse

Table 4.

Disturbances due to elevator deflection

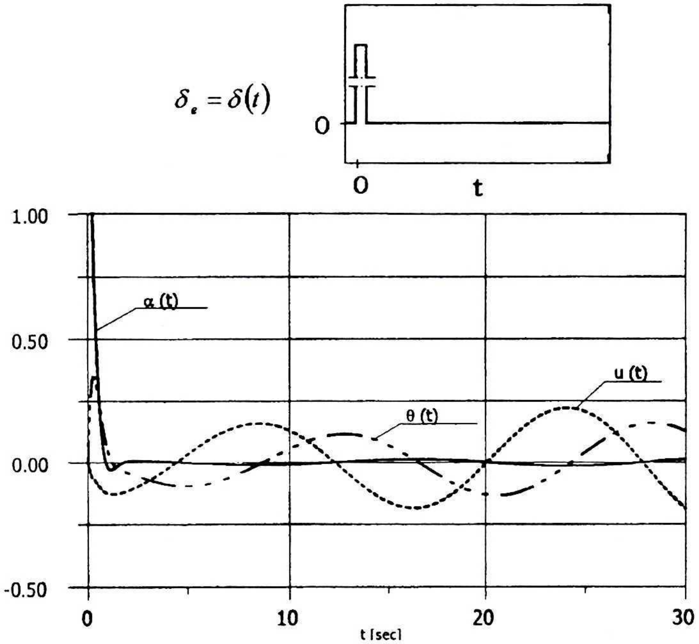

Fig. 9. Excitation by Dirac impulse

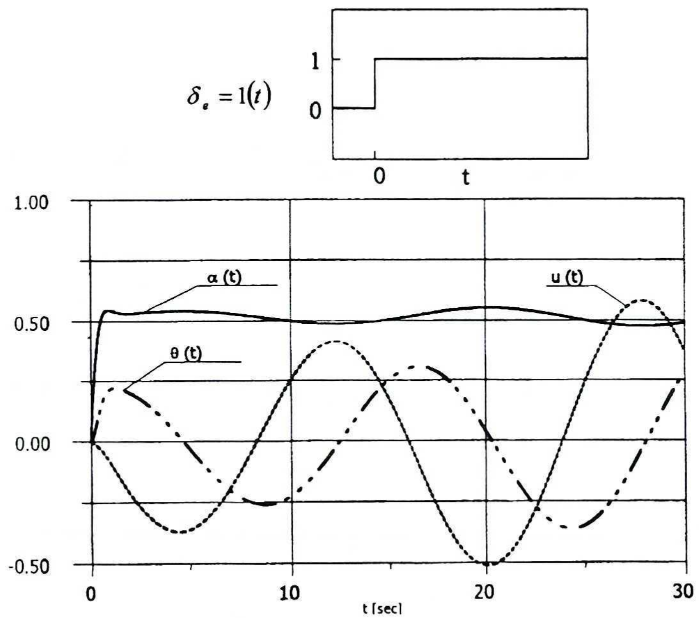

Fig. 10. Excitation by Heviside function

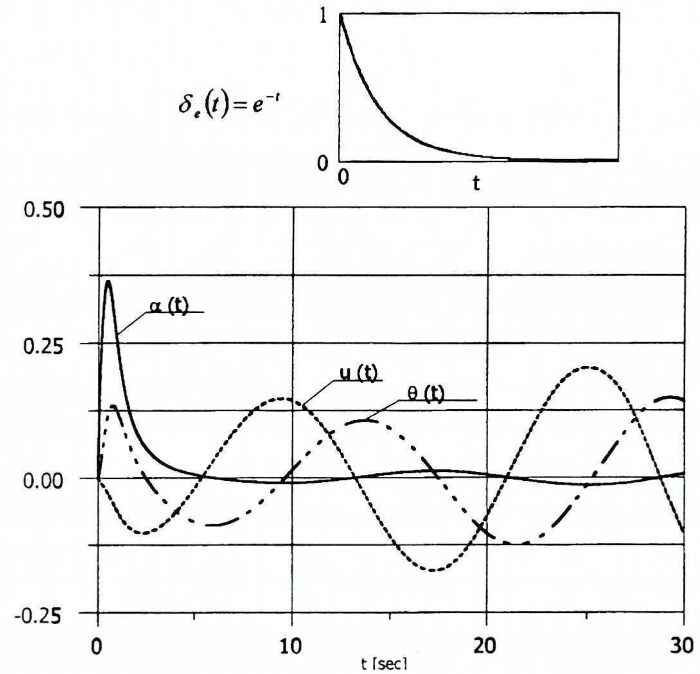

Fig. 11. Exponential impulse

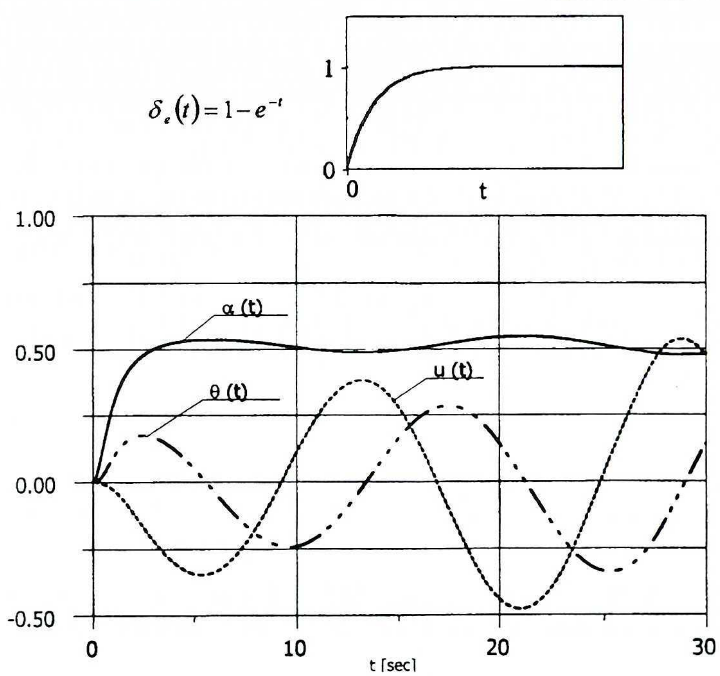

Fig. 12. Unit minus exponential impulse

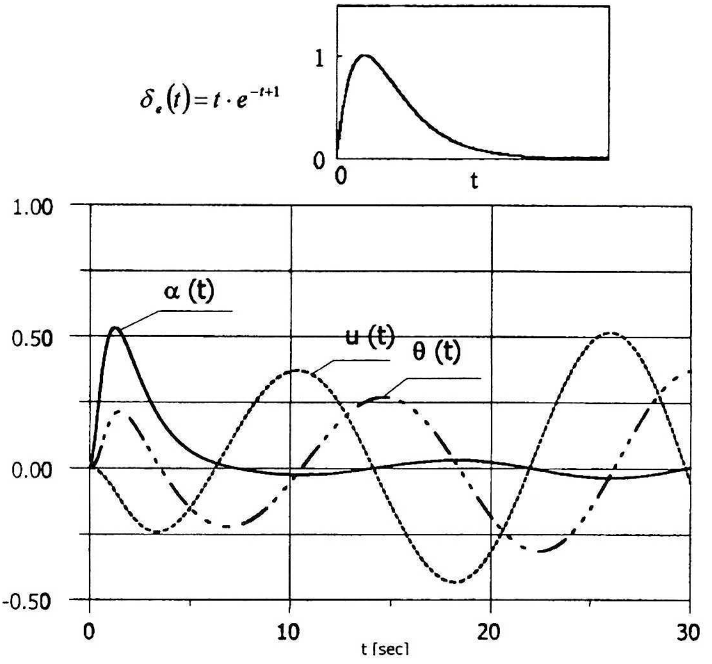

Fig. 13. Complex impulse

5. Conclusions

Presented results have been obtained under the assumption that glider is a perfectly stiff, rigid body. Aspect ratio of PW-5 is about 18, and the main structure is made of a glass-epoxy composite, which is relatively flexible material. Moreover, the algorithm of calculations (Laplace transform) used here – although very convenient – makes it possible to solve equations of motion for small disturbances only. More intense disturbances should be a subject of non-linear analysis and were not considered here. An advantage of the method used here is decomposition of complex input signal into a number of simpler ones (for example harmonic), that can be analysed easy. Once the all partial solutions are found, the response of glider can be obtained using the principle of superposition.

Bode plots show that dynamic characteristics depend strongly on frequencies of disturbances. Such a dynamic analysis performed at the early stage of design process enables the designer to shape those characteristics intentionally instead of performing a 'post factum' analysis. The aims to be reached are not only better control characteristics but also extended fatique durability of the glider, improvements of flight comfort and – regarding high-performance gliders – making better use of thermal air currents during cross-country flights (especially in application to the dolphin shape flight).

Manuscript received by Editorial Board, July 28, 2000;
final version, September 23, 2000.

REFERENCES

[1] Roskam J.: Flight Dynamics and Automatic Control Systems. vol. I, II, DAR Corporation, Kansas 1995.

[2] Cook M.V.: Flight Dynamics Principles. Arnold, London 1997.

[3] Hancock G.J.: An Introduction To The Flight Dynamic of Rigid Aeroplanes. Elis Horwood, London 1995.

[4] Kuo B.: Automatic Control Systems. Prentice-Hall International, London 1991.

[5] Goraj Z.: Calculations of Manoeuvrability and Stability of an Aircraft in Subsonic Flow. Warsaw University of Technology Publications, Warsaw 1984, in Polish.

[6] Goraj Z.: Calculations of Static Stability and Manoeuvrability of an Aircraft. Warsaw University of Technology, Warsaw 1985, Lecture in Flight Dynamics, in Polish, unpublished.

[7] Goraj Z.: STB-9702 – Software Package for Calculations of Static Manoeuvrability and Stability and Flight Dynamics of an Aircraft. Warsaw University of Technology, Warsaw 1997, unpublished.

[8] The PW-5 Glider Data Sheet. Warsaw University of Technology, Warsaw 1994, in Polish, unpublished.

[9] Stability of the PW-5 Glider with Centre of Gravity at 43% Mean Aerodynamic Chord. Warsaw University of Technology, Warsaw 1993, in Polish, unpublished.

[10] The PW-5 Glider Loads on Structure. Warsaw University of Technology, Warsaw 1993, in Polish, unpublished.

Dynamiczna analiza ruchu szybowca w płaszczyźnie symetrii – przypadek szybowca PW-5

Streszczenie

W pracy przedstawiono analizę stateczności dynamicznej szybowca klasy światowej PW-5 „Smyk". Założono, że szybowiec jest bryłą sztywną i posiada trzy stopnie swobody – dwa przesunięcia i jeden obrót w płaszczyźnie symetrii bryły. Wyznaczono odpowiedź szybowca na wymuszenia pochodzące od podmuchu oraz wychylenia steru wysokości.

Dokonano algebraizacji różniczkowych równań ruchu poprzez zastosowanie transformacji Laplace'a. Wyznaczono funkcje przejścia układu, które po zadaniu sygnałów wejściowych, a następnie wykonaniu transformacji odwrotnych pozwoliły na wyznaczenie przebiegów odpowiedzi szybowca w funkcji czasu. Stosowano proste sygnały wejściowe, tak aby możliwe było znalezienie transformaty odwrotnej w postaci zamkniętej.

Pomimo dość silnych założeń przyjętych w pracy (bryła sztywna, małe zaburzenia pozwalające na analizę liniową) przedstawione wyniki są oryginalne i nie były dotychczas publikowane. Przepisy budowy szybowców (JAR, FAR) nie wymagają przeprowadzenia analiz dynamicznych szybowca. W celu dopuszczenia szybowca do prób w locie i uzyskania certyfikatu typu wymagane jest jedynie dowiedzenie stateczności statycznej. Dynamika szybowca oceniana jest w trakcie prób jedynie jakościowo, w formie subiektywnej opinii pilotów doświadczalnych.